

# IMPROVED REPEATABILITY FOR CALIBRATION OF SHOCK ACCELEROMETERS

Lixue Wu

Institute for National Measurement Standards, National Research Council Canada  
1200 Montreal Rd., Ottawa, Ontario, Canada K1A 0R6

## 1. INTRODUCTION

A previous study of the NRC system for calibration of shock accelerometers investigated the effect of mass loading on the system using a vibrometer [1]. At that time, the repeatability of the measurements was limited by the resolution of the instrumentation in use. Further investigation of the effect of mass loading effect will use improved instrumentation: a reference accelerometer replaces the vibrometer for sensing the shock pulse motion, and a high-speed and high-resolution (14-bit) A/D conversion card is used to record the waveforms of the outputs of the accelerometers. This paper describes the signal processing techniques that can then be applied to the recorded waveforms to extract acceleration peak values.

## 2. CALIBRATION METHOD

An upward-moving pneumatically-operated projectile, as illustrated in Fig. 1, provides a simple means for the comparison shock calibration of accelerometers. A pressure release mechanism controls the moving speed of the projectile. The shock acceleration is created by the projectile impacting on an anvil that has pads attached to its bottom surface. A wide range of shock pulse amplitudes and durations can be generated by controlling the drive pressure and the mass of the target (anvil and accelerometers).

### 2.1 Mass loading

Mass loading affects the sensitivity of an accelerometer. In order to calibrate the accelerometer under test for a particular load, dummy masses (steel cylinders) can be mounted using studs between the accelerometer under test and the reference accelerometer (refer to Fig. 1). The mass loading effect can be corrected if mass loading correction curves are published by manufacturers [1]. These curves, however, may not be applicable to shock acceleration.

A torque wrench is used to secure the mass and accelerometers to the anvil with a specified torque (typically 2 N·m). In this arrangement the top accelerometer has no mass load and the bottom accelerometer is loaded by a mass that is the sum of the cylinder mass and the mass of the top accelerometer.

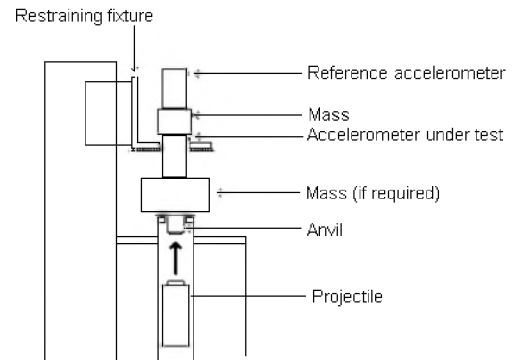


Fig. 1. Arrangement for shock accelerometer calibration.

### 2.2 Accelerometer sensitivity

Let  $S_t(a, m)$  and  $S_b(a, m)$  be the voltage sensitivities at shock amplitude  $a$  and mass load  $m$  for the top and bottom accelerometer including charge amplifiers, respectively. Let  $V_t$  and  $V_b$  be the peak voltage outputs of the charge amplifiers for the top and bottom accelerometers, respectively. Assume that  $S_t(a_i, 0)$  is known. (The reference accelerometer is calibrated at discrete shock amplitudes with no mass load.) Since  $V_t = a S_t(a, 0)$ , one can control the drive pressure to the projectile to achieve  $a_i = V_t / S_t(a_i, 0)$  within a predefined tolerance. Further assume that the assembly of the mass load and the accelerometers is rigid enough that relative motion between the top and bottom accelerometer is negligible. Thus, the output of the charge amplifier for the bottom accelerometer is given by  $V_b = a_i S_b(a_i, m)$ . That is,

$$S_b(a_i, m) = S_t(a_i, 0) V_b / V_t.$$

### 2.3 Instrumentation

The instrumentation used to measure the ratio of the peak voltage outputs is shown in Fig. 2. The trigger of the digitizer is set to upward slope and one half of the expected pulse amplitude. The trigger event position is set to 50% (designating 50% of the record length to be pre-trigger samples and 50% of the record length to be post-trigger samples). Using this setting, any DC bias of the output signal can be detected from the pre-trigger samples and then removed.

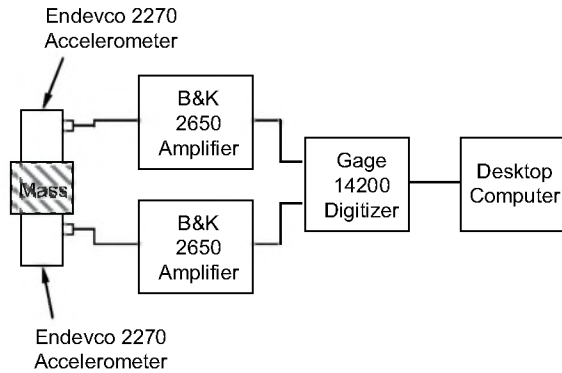


Fig. 2. Arrangement of instrumentation.

### 2.4 Measurement repeatability

The repeatability of the measurement of peak voltage ratio  $V_b/V_t$  is one of the major contributions to the measurement uncertainty of  $V_b/V_t$ . Therefore, signal processing methods for processing the recorded signals to improve three aspects of the voltage ratio measurement have been investigated.

#### DC bias

DC bias exists in recorded signals. With no motion (except environmental vibrations) on accelerometers, the outputs of the charge amplifiers were recorded by the digitizer and further studied for the time variance of the DC bias. It was found that DC bias remains almost constant over a period of equal to the length of the shock pulse (a few milliseconds). Thus, the DC bias estimated from the pre-trigger samples (corresponding to no accelerometer motion) can be used to correct for the DC bias in the post-trigger samples.

#### Waveform distortion

Damage to the pads which are attached to the bottom of the anvil causes distortion in the shock waveforms and therefore contributes to the poor repeatability of the voltage ratio measurements. The damage to the pads is not always visible. A likelihood test is therefore used to examine the similarity of two pulses recorded. One of the pulses is rescaled and time-shifted to compensate for the gain- and phase-differences between the two measuring channels. The minimum mean squared error between the two waveforms is then calculated for optimal scale factor and time shift. This minimum mean squared error is then compared to a preset limit to decide whether the recorded signals are acceptable.

#### Noise

Environmental noise (such as external vibration and the interference from power line or radio frequency sources) and inherent noise (such as Johnson and preamplifier noise) also contribute to the poor repeatability

of the voltage ratio measurements. Band pass filters can be used to remove noise to some extent. To further reduce the effect of noise, a polynomial function of variable order is applied to model the waveform around the peak of the pulse. The model parameters (polynomial coefficients) are found by minimising the mean squared error between the polynomial function and the recorded waveform. The peak value is then calculated using the polynomial function.

## 3. RESULTS

Shown in Fig. 3 are example plots of recorded waveforms and their polynomial model functions (in dark lines). The one having lower peak is the output from the reference accelerometer.

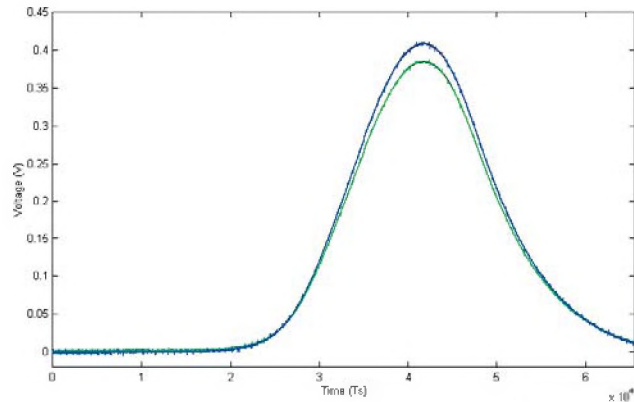


Fig. 3. Plots of recorded waveforms and their model functions, where  $T_s$  is the sampling interval and  $T_s = 1/50 \mu s$ .

The measurement data for ten voltage ratio measurements are listed in Table 1. The standard deviation of the measurements  $V_b/V_t$  is 0.016 % with shock amplitudes controlled within  $\pm 0.75$  % of  $a_t$  for a mass load of 40 g.

Table 1. Measurement data for mass load of 40 g

$V_t$	$V_b$	$V_b/V_t$	$V_t$	$V_b$	$V_b/V_t$
0.3839	0.4077	1.0620	0.3838	0.4077	1.0622
0.3836	0.4073	1.0618	0.3854	0.4093	1.0619
0.3829	0.4066	1.0619	0.3864	0.4104	1.0621
0.3877	0.4118	1.0622	0.3836	0.4074	1.0620
0.3857	0.4097	1.0623	0.3858	0.4096	1.0618

## 4. CONCLUSION

In the previous study of mass loading effect, the variance of the measured shock sensitivity was up to 1 %. Replacing the 8-bit A/D converter by the 14-bit digitizer and implementing the three signal processing methods reduces the variance of the measured shock sensitivity significantly.

## REFERENCES

- [1] Wu, L., Wong, G.S.K., Hanes, P., Ohm, W.S. (2004). The effect of mass loading on the sensitivity of shock accelerometers. *Canadian Acoustics*, 32 (3), 96-97.
- [2] Sill, Robert D. Mass loading in back-to-back reference accelerometers. Technical Paper 310, Endevco Corporation.